Capture of Negative Muons by Nuclei*†

J. C. SENS‡
The Enrico Fermi Institute for Nuclear Studies, The University of Chicago, Chicago, Illinois
(Received September 8, 1958)

An experiment conducted to obtain precise values for the rates at which negative muons are captured by nuclei is described. These capture rates were deduced from muon disappearance rates measured by determining the time distribution of electrons resulting from the decay of muons in their lowest atomic orbit. 30 elements were investigated, using scintillation counters as detectors. The data are compared with the general theory of Primakoff and the specific predictions of Tolhoek and Luyten for nuclei with $20 \leq Z \leq 28$. Primakoff's predictions for the effect of the Pauli principle are well borne out by this experiment, and the inferred capture rate of muons by protons is in good agreement with the hypothesis of a universal Fermi interaction. New values of effective nuclear charge densities (analogous to Wheeler's Z_{eff}[4]) were computed for analyzing the data, using a recent muon mass and up-to-date experimental information on charge distributions (from electron scattering and mesonic x-ray work). These new values are presented in tabular form.

I. INTRODUCTION

A. Purpose of the Experiment

THE purpose of the experiment here described is to determine with high accuracy the rates at which negative muons are captured by nuclei from their lowest atomic orbits.[1]

According to our present knowledge, there are three processes in which the negative muons, once stopped in matter, participate: (a) electromagnetic interactions, (b) the decay into an electron and two neutrinos, and (c) capture by nuclei. The decay process is slow and, since the experiments of Conversi *et al.*, and of others,[2] it is known that the capture process can likewise be classified as a "weak" interaction. This process is of the form $\mu^- + p \rightarrow n + \nu$, as follows from the absence of charged particles and gamma rays among the final products, and from the kinematics of the reaction.[3] The similarity between this process and the β decay of the muon and the neutron is suggestive of a possible "universal Fermi interaction" (UFI) between the pairs of spin-$\frac{1}{2}$ particles, np, $\mu\nu$, $e\nu$,[4] and possibly others.[5] The problem is in particular to determine both the *types* of coupling and the interaction *strengths* for these processes. In the case of the neutron and muon decays, the interaction is now believed to be a mixture of V and A,[6] and to have coupling constants which are of the same order of magnitude (2 to 3×10^{-49} erg cm^3). It is therefore of interest to determine whether this type of coupling, with the same strength, can explain the experimental evidence regarding muon capture as well. On the other hand, the assumption of UFI may, strictly speaking, be valid only for "bare" particles, and not for the physical nucleons (which can, e.g., interact via pions) involved in neutron decay and muon capture. Thus an empirical test of the UFI may indicate whether renormalization effects (which may change the over-all strengths of the couplings as well as their type) are important or not.

The object of the present experiment is thus twofold. In the first place we want to infer by experiments with complex nuclei the strength of the coupling which is operative in the elementary capture process $\mu^- + p \rightarrow n + \nu$. Previous measurements indicate that this coupling strength is of the same order of magnitude as the one in β decay.[7] The experiment to be described here confirms this result with improved accuracy. Secondly, by measuring muon absorption in several nuclei, the specific dependence on the type of interaction, and on Z, can be studied. The very simplest model predicts a capture probability proportional to Z^4; it is based on the assumption that all protons can interact independently with the muon in the K orbit, that the nucleus is a point, and that the interaction is proportional to the muon density at the position of the

* Research supported by a joint program of the Office of Naval Research and the U. S. Atomic Energy Commission.
† A thesis submitted to the Department of Physics, the University of Chicago, in partial fulfillment of the requirements for the Ph.D. degree.
‡ Present address: CERN, Geneva, Switzerland.
[1] A preliminary account of the results is given by J. C. Sens *et al.*, Phys. Rev. **107**, 1464 (1957).
[2] Conversi, Pancini, and Piccioni, Nuovo cimento **3**, 372 (1947); T. Sigurgeirsson and K. A. Yamakawa, Phys. Rev. **71**, 319 (1947); G. E. Valley, Phys. Rev. **72**, 772 (1947).
[3] For a survey of the arguments, see R. D. Sard and M. F. Crouch, in *Progress in Cosmic-Ray Physics*, edited by J. G. Wilson (North-Holland Publishing Company, Amsterdam, 1954), Vol. 2.
[4] G. Puppi, Nuovo cimento **5**, 587 (1948); J. Tiomno and J. A. Wheeler, Revs. Modern Phys. **21**, 153 (1949); Lee, Rosenbluth, and Yang, Phys. Rev. **75**, 905 (1949); C. N. Yang and J. Tiomno, Phys. Rev. **79**, 495 (1950).
[5] M. Gell-Mann and A. H. Rosenfeld, *Annual Review of Nuclear Science* (Annual Reviews, Inc., Stanford, 1957), Vol. 7, p. 407.
[6] E. C. G. Sudershan and R. E. Marshak, Proceedings of the Padua-Venice Conference, September, 1957 (Suppl. Nuovo cimento, to be published); Phys. Rev. **109**, 1860 (1958); R. P. Feynman and M. Gell-Mann, Phys. Rev. **109**, 193 (1958); J. J. Sakurai, Nuovo cimento **7**, 649 (1958).
[7] J. W. Keuffel *et al.*, Phys. Rev. **87**, 942 (1952); H. K. Ticho, Phys. Rev. **84**, 1337 (1948); L. Lederman and M. Weinrich, *Proceedings of the CERN Symposium on High-Energy Accelerators and Pion Physics, Geneva, 1956* (European Organization of Nuclear Research, Geneva, 1956); N. N. Biswas, Trans. Bose Research Inst. Calcutta **19**, 79 (1953–55); D. R. Jones, Phys. Rev. **105**, 1591 (1957).

nucleus,[8]

$$\sum_Z |\psi_\mu(0)|^2 = Z|\psi_\mu(0)|^2 = Z^4/\pi a_0^3, \quad (1)$$

with a_0 as the muon Bohr radius, and $\psi_\mu(0)$ the K-orbit wave function for the muon, evaluated at the origin. These assumptions are clearly too crude, in particular for high Z where the radius of the muon orbit is comparable to the nuclear radius. For a nucleus of finite size with a continuous charge distribution, the capture rate is proportional to

$$\langle\rho\rangle = \frac{\left|\int_0^\infty \int_0^\infty \psi_P(x)\psi_\mu(x')\delta(x-x')d^3x d^3x'\right|}{\int_0^\infty |\psi_\mu(x')|^2 d^3x'} = \frac{\int_0^\infty \rho(x')|\psi_\mu(x')|^2 d^3x'}{\int_0^\infty |\psi_\mu(x')|^2 d^3x'}, \quad (2)$$

which defines the effective charge density $\langle\rho\rangle$. By expressing $\langle\rho\rangle$ in terms of the square of the hydrogenic wave function at the origin, one obtains Wheeler's expression for Z_{eff}:

$$\pi a_0^3\langle\rho\rangle = Z_{\text{eff}}^4. \quad (3)$$

If, in particular, the charge distribution is assumed to be uniform, we have

$$Z_{\text{eff}} = \left[\pi a_0^3 \frac{Z}{\frac{4}{3}\pi R^3} \frac{\int_0^R |\psi_\mu(x)|^2 d^3x}{\int_0^\infty |\psi_\mu(x)|^2 d^3x}\right]^{\frac{1}{4}} = C\left[\frac{Z}{A}\frac{\int_0^R |\psi_\mu(x)|^2 d^3x}{\int_0^\infty |\psi_\mu(x)|^2 d^3x}\right]^{\frac{1}{4}}, \quad (4)$$

where R = nuclear radius.

Wheeler has evaluated Eq. (4) for several nuclei, using ground state wave functions of the 3-dimensional isotropic oscillator, force constants derived from $R = (e^2/2m_e c^2)A^{\frac{1}{3}}$, and $m_\mu = 210 m_e$ (this gives $C = 47.1$). There is strong disagreement with experiment for high Z.

Primakoff[9] has calculated the capture process taking into account that, owing to the Pauli principle, there is a limitation in available final states for the neutron. He uses the closure approximation to sum over the final states and obtains the following expression for the capture rate by a nucleus (A,Z):

$$\Lambda_{\text{cap}}(A,Z) = \gamma\Lambda_{\text{cap}}(1,1)Z_{\text{eff}}^4[1-(A-Z)\delta/2A], \quad (5)$$

when terms of order $1/A$ are neglected. It is to be noted that while a completely arbitrary mixture of S, V, T, and A couplings is admitted at the outset of the calculation, the result (5) is insensitive—precisely to terms of order of $1/A$—to the exact nature of the interaction. The capture rate depends, apart from $\Lambda(1,1)$, on two parameters, δ and γ. The exclusion principle manifests itself through the last bracket, where the fractional neutron excess $(A-Z)/2A$ appears multiplied by a nucleon correlation parameter δ. The parameter γ accounts for the reduction in available neutrino phase space which is due to binding of the neutron in complex nuclei, as well as for nucleon recoil effects. Primakoff estimates $\delta \approx 3$ and $\gamma \approx 0.73$ from nuclear data. Formula (5) is, with fixed values of these parameters, supposed to hold *in the mean* rather than exactly for each given (A,Z).

Assuming UFI, i.e., that in muon capture

$$(\sum c_i^2)^{\frac{1}{2}} \equiv (|c_S|^2 + |c_V|^2 + 3|c_T|^2 + 3|c_A|^2)^{\frac{1}{2}} = 3.2\times 10^{-49} \text{ erg cm}^3, \quad (6)$$

namely that the *effective* sum of squared coupling constants is numerically equal to the corresponding sum in the β decay of the free neutron (where[10] $ft^{\frac{1}{2}} = 708 \pm 20$ sec, $W_0 = 2.53\ m_e c^2$, $ft^{\frac{1}{2}} = 1170 \pm 36$), one predicts

$$\Lambda_{\text{cap}}(1,1) = (209\pm 6) \text{ sec}^{-1}, \quad (7)$$

using the formula

$$\Lambda_{\text{cap}}(1,1) = \frac{1}{2\pi^2}\left(\frac{1}{137}\right)^3 \frac{m_\mu^5 c^4}{\hbar^7} R(\sum c_i^2), \quad (8)$$

with

$$R = (1-m_\mu/m_N)/(1+m_\mu/m_N) = 0.77.$$

It should be mentioned that $\Lambda(1,1)$ in (5) and obtained above is *not* the actual rate, $\Lambda_{\text{cap}}^{\text{phys}}(1,1)$, at which muons would be captured from $1s$ orbits by protons. This rate is given by

$$\Lambda_{\text{cap}}^{\text{phys}}(1,1) = \Lambda_{\text{cap}}(1,1)\mu^3, \quad (9)$$

where

$$\mu = m_\mu^{\text{red}}/m_\mu = (1+m_\mu/m_P)^{-1} = 0.898.$$

Tolhoek and Luyten[11] have made explicit calculations for the nuclei with $20 \leq Z \leq 28$. Their approach differs from that of Primakoff in that here specific initial and final shell model states are considered and that separate

[8] J. A. Wheeler, Revs. Modern Phys. **21**, 133 (1949).

[9] H. Primakoff (private communication) and *Proceedings of the Fifth Annual Rochester Conference on High-Energy Physics* (Interscience Publishers, Inc., New York, 1955), p. 174.

[10] Sosnovskii, Spivak, Prokofiev, Kutikov, and Dobrynin, *1958 Annual International Conference on High-Energy Physics at CERN*, edited by B. Ferretti (CERN, Geneva, 1958). In using Eq. (6) to test UFI, we implicitly assume (a) 2-component neutrinos, and (b) the absence of Fierz terms, for both of the processes we compare.

[11] H. A. Tolhoek and J. R. Luyten, Nuclear Phys. **3**, No. 5, 679 (1957).

calculations are made for the S,V and T,A interactions.

The second purpose of this experiment is then to confront the theories of Primakoff, and of Tolhoek and Luyten with the measured capture rates. To this end, both nuclei in the range $20 \leq Z \leq 28$ and those on either end of the periodic table were studied.

In the following, a few remarks will be made about the methods by which nuclear interactions of negative muons can be detected. In Sec. II, the experiment will be described and the data analyzed. Section III contains a brief discussion of the results.

B. Methods of Detection

Muons, entering a target material, are slowed down to a velocity of the order of that of the valence electrons in a time of less than 10^{-9} sec. They then cascade down to the lowest orbits of the mesonic atoms, in times of the order of 10^{-13} sec,[12] from where they disappear either by decay into an electron and two neutrinos or through capture by the nucleus. The total rate of disappearance of muons, Λ_t, is thus

$$\Lambda_t = \Lambda_d^- + \Lambda_{\text{cap}}, \tag{10}$$

where Λ_d^- = rate of decay and Λ_{cap} = rate of capture. In the capture process, the muon rest energy is partly carried off by the neutrino, and partly used for excitation of the nucleus with subsequent emission of γ rays, neutrons, and possibly internal conversion electrons and charged particles.

If one assumes that the decay rate from a bound orbit, Λ_d^-, is the same as that of a positive (free) muon, Λ_d^+, then Λ_{cap} can be determined either (1) by measuring the time distribution of the decay electrons and/or capture products (γ rays and neutrons) which emerge from the target after arrival of the muon; or (2) indirectly, by counting electrons in a "gate" which is opened a given time after arrival of the muon and closed some suitable time (for optimum electron to background yield) later.

The validity of the above made assumption that $\Lambda_d^- = \Lambda_d^+$ can be tested in the following way. If N_e electrons are counted from a target in which N_μ muons have been stopped, then

$$N_{e\mu} \equiv N_e/N_\mu = \epsilon \Lambda_d/\Lambda_t, \tag{11}$$

where ϵ is the efficiency for counting electrons, as determined by the counter geometry and the absorption in the target. Determination of Λ_t and $N_{e\mu}$ then gives Λ_d^-, once ϵ^- has been either measured or eliminated. A recent investigation of this point[13] has revealed that Λ_d^- is *not* equal to Λ_d^+, but can differ from it by as much as 50%.

The first method of determining Λ_{cap} has not only the obvious advantage of giving more information per event, due to a division of the time scale into smaller units, but is also less sensitive to the substitution Λ_d^+ for Λ_d^- in (10) than the method of counting the electron yield in a wide gate. This can be seen as follows. Define R as $\Lambda_d^- = R\Lambda_d^+$. The ratio of gate counts in two elements is then, from (11):

$$\frac{N_{e\mu}(Z_1)}{N_{e\mu}(Z_2)} \sim \frac{1}{R} \frac{\Lambda_t(Z_2)}{\Lambda_t(Z_1)}, \tag{12}$$

assuming that $\Lambda_d^-(Z_1) \approx \Lambda_d^+$, i.e., that Z_1 is low. It then follows that the relative error in the capture rate introduced by disregarding the effect of binding is given by

$$\left| \frac{\Delta\Lambda_{\text{cap}}(Z_2)}{\Lambda_{\text{cap}}(Z_2)} \right| = \frac{|1-R|}{R}, \tag{13}$$

whereas, if one measures $\Lambda_t(Z_2)$ directly

$$\left| \frac{\Delta\Lambda_{\text{cap}}(Z_2)}{\Lambda_{\text{cap}}(Z_2)} \right| = \frac{|1-R|}{R} \frac{\Lambda_d^+}{\Lambda_t/R - \Lambda_d^+}. \tag{14}$$

For the case of Cd, for example, where $R \cong 0.9$, (13) gives 11%, while (14) gives 0.5%.

In this experiment Λ_t is measured directly. The time distribution of the decay electrons is determined by feeding the muon and electron signals into a time-to-pulse height-converter; the height of the output signal of the latter is proportional to the time delay between muon and electron. This signal is then measured and stored in a 100-channel pulse-height analyzer.

II. EXPERIMENT

A. Description of the Apparatus

A beam of negative mesons (70% pions, 10% muons, 20% electrons) of momentum 145 Mev/c is extracted from the synchrocyclotron. The muon/pion ratio is increased in the customary way[14] from 1/7 to 7/1. The muon beam so prepared (see Fig. 1) goes through a sufficient amount of Cu (28.2 g/cm^2 for most targets) to stop the residual pions and to center the muon range in the targets. The position of the various counters with respect to the target is shown in Fig. 2. The counters consist of plastic scintillators which are connected to Lucite light pipes and RCA-6810 photomultipliers.

Measurements were performed on 30 targets. Twenty-six elements and 4 compounds were prepared in various forms. A typical target had an area of about 80 cm^2, in view of a beam diameter of approximately 9 cm. The target thicknesses ranged from 6 to 12 g/cm^2. Polyethylene bags of negligible thickness were used to contain lump-shaped or powder targets. The chemical purity of all targets was better than 97.6%.

Figure 3 gives a diagram of the electronics. The beam is monitored by a (1,2) coincidence; a muon stopped in

[12] E. Fermi and E. Teller, Phys. Rev. **72**, 399 (1947).

[13] Lundy, Sens, Swanson, Telegdi, and Yonanovitch, Phys. Rev. Letters **1**, 102 (1958).

[14] N. Campbell and R. A. Swanson (unpublished report).

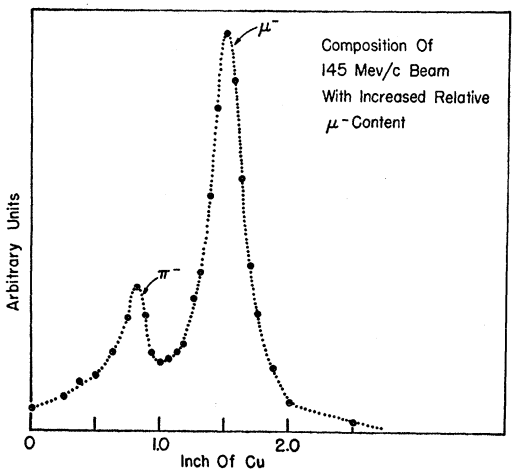

FIG. 1. Differential range curve of the meson beam used.

the target is registered as a $(1,2,3,\bar{4})$ event (the bar indicating an anticoincidence); the electron or nuclear gamma ray is defined as a $(\bar{3},4,5)$ event. The coincidences and anticoincidences are made in Garwin-type circuits,[15] followed by a trigger circuit[16] capable of high repetition rate. The anticoincidence efficiency is checked to be better than 99.9%.

The time elapsed between the muon telescope signal and the electron telescope signal is measured in a time-to-pulse height-converter. The time converter (T.C.) is a design of Weber *et al.*[17] as modified by K. H. Benford. This modification is discussed by Swanson.[18] The essential feature is illustrated in Fig. 4. In the original version the plate current in the tube (6BN6) is turned on by the "start signal" and keeps flowing until the "stop signal" has arrived. During this time the plate voltage drops linearly at a rate i_p/C. After the stop signal has cut off the tube, C is recharged with a time constant RC ($\approx$600 μsec). In the modified version, the RC circuit decays for the duration of the muon-electron delay while the recharging takes place with a time constant $C/g_m \approx 5$ μsec. Contrary to the actual sequence of events, the T.C. is started with the electron pulse and stopped with the muon signal. To this end, the muon telescope output passes through a delay line before entering the stop side. The number of $(\bar{3},4,5)$ events decreases from 36% (low-Z elements) to 5% (high-Z) of the $(1,2,3,\bar{4})$ rate. Since a start pulse without a stop pulse produces an output signal, while a stop pulse without a start pulse does not, losses due to the finite (400 μsec) recovery time of the pulse-height analyzer (P.H.A.) following the T.C. are reduced by feeding the least frequent signal into the start side. The losses are reduced at the beam rates used (see below) by this reversed operation from 40% to 20% for a low-Z element, and from 75% to less than 1% for high Z. (The output is fed into a linear amplifier and from there into the P.H.A.)

Three T.C. ranges, of usable lengths 6.4, 2.9, and 0.9 μsec, were used. Each range is determined by the length of the shorted line in the pulse-shaping portion of the start side, and the delay between muon telescope and stop side. Switching ranges is done by changing these two lines and by adjusting slope and size of the output pulse in such a way that in all cases the total time-span covers nearly the full P.H.A. range (8 volts). The delay between the muon telescope and the stop side is made slightly shorter than the shorted line in the start side of the T.C.; start pulses, not accompanied by stop pulses, so-called "uncorrelated events," will than appear in a higher channel of the P.H.A. than "prompt events." This feature is essential for the analysis of composite lifetimes.

The T.C. is calibrated and a check on the over-all linearity of time converter, amplifier, and P.H.A. is made by admitting simultaneous pulses to the electron and muon telescopes and delaying the start pulse by means of a variable calibrated delay line. The target is removed, so that the beam traverses all counters, and the telescopes are now set for coincidences only $[(4,5)$ respectively $(1,2,3)]$. The calibration is determined to better than 1%. Deviations from linearity and absolute stability of more than 1% have not been observed.

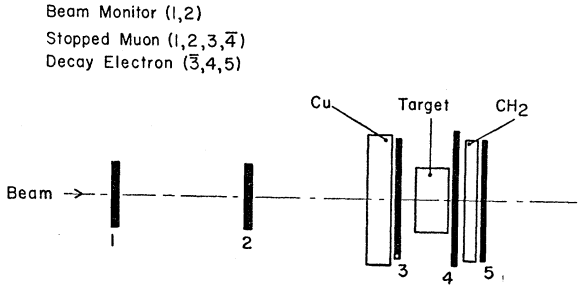

FIG. 2. Experimental arrangement for the capture experiment.

In the geometry of this experiment, characteristic yields per hour were (1) for low Z, 2×10^5 stopped μ's, 35×10^3 correlated electrons, 1.3×10^3 background counts over a 1-μsec time interval; (2) for high Z, 8×10^5 stopped μ's, 10^3 correlated electrons, 3×10^3 background counts over a 1-μsec time interval. From a run with positive muons an efficiency for counting positrons of $\approx$18% was found; this efficiency is determined both by geometrical factors and losses due to positrons stopping in the target.

B. Analysis of the Data

The electron time distributions observed with elemental targets were analyzed as follows. The time

[15] R. L. Garwin, Rev. Sci. Instr. 24, 618 (1953).
[16] W. C. Davidon and R. B. Frank, Rev. Sci. Instr. 27, 15 (1956).
[17] Weber, Johnstone, and Cranberg, Rev. Sci. Instr. 27, 166 (1956).
[18] R. A. Swanson, Phys. Rev. 112, 580 (1958).

(i.e., pulse-height) scale was divided into intervals of width d. The counts in each interval were added and assigned to the center of the interval. From the data at times $t>3\tau$ which contained $<5\%$ correlated electrons, an estimate of the background was made; this background is due mainly to electrons accidentally correlated with a muon. After subtraction of a background rate constant in time, the mean life for disappearance, $\tau=\Lambda_t^{-1}$, was determined by the method of Peierls.[19] The choice $d<0.3\tau$ was made in all cases, so that it was sufficient to carry out the calculations to first order. In order to minimize statistical errors (see below), the analysis was performed on electrons occurring over a total time interval T such that $2.7\tau<T<4.4\tau$.

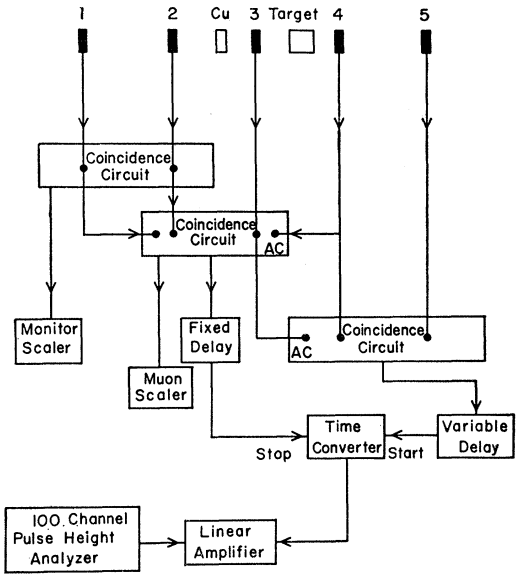

FIG. 3. Block diagram of the electronics.

The errors were evaluated in the following manner. If the measured distribution were a pure exponential, extending to $t=\infty$, the error in the mean life due to statistics would be $(\delta\tau/\tau)=1/N^{\frac{1}{2}}$, where N is the total number of analyzed counts. The presence of a constant background and a cutoff on the time scale enhances this error by a factor $(A+B/\beta)^{\frac{1}{2}}$, where A and B are constant for a given T/τ and β is the ratio, at $t=0$, of the rate to the background rate. For a given β, this factor is minimum for T/τ around 3.5. The errors, calculated in this way, range from 0.5% (low Z) to 6% (high Z). The T.C. calibration was drift-free and linear to 1% and therefore contributed an error of this magnitude. Finally, in evaluating Λ_{cap} from Λ_t, an error of 1% in Λ_d ($\tau_d=2.21\pm0.02$ μsec) has been included.

The capture rates, Λ_{cap}, thus obtained have further to be corrected for two effects:

(1) The effect of uncorrelated stop pulses in the time converter. The T.C. measures the time elapsed between an electron and the first muon following it, whether this is the parent muon or an accidental. Consequently, the time distribution in the presence of a stop rate M is given by

$$e^{Mt}(Ae^{-\Lambda_t t}+C), \tag{15}$$

as shown by Swanson.[18] M is the instantaneous muon stop rate; A is a constant, and C may be taken as such since it was established experimentally that its time dependence was less than 5% in most cases, while C itself was about 10% of the electron rate in the first interval. The correction is thus

$$\Lambda_t=\Lambda_t'+M, \tag{16}$$

where Λ_t is the true muon disappearance rate [in the absence of correction (2)] and Λ_t' the observed rate.

(2) The effect of precession in a magnetic field. As is well known,[20] parity nonconservation affects both the production and the decay process of the muon: it results in the production of longitudinally polarized muons, while its effect on the decay is exhibited in an asymmetry in the angular distribution of the electrons with respect to the muon spin. A vertical magnetic field will cause the muon to precess, with the result that the time distribution observed in the electron telescope is, instead of just $N(t)=N_0e^{-\Lambda_t t}$,

$$\tilde{N}(t)=N_0e^{-\Lambda_t t}(1-a\cos\omega t)=N_0\exp(-\tilde{\Lambda}_t t), \tag{17}$$

with $\omega=g(e/2m_\mu c)B$.[21] The change in Λ_t, $\Delta\Lambda_t$, is then roughly given by

$$\frac{\Delta\Lambda_t}{\Lambda_t}=\frac{1}{\Lambda_t}\left(\frac{a}{1-a}\right)\left(\frac{1-\cos\omega t'}{t'}\right), \tag{18}$$

where t' is the time interval over which $\tilde{\Lambda}_t$ and Λ_t are evaluated. Equation (18) does not take into account the fact that the "early" points carry more weight than the later ones. An explicit evaluation by the method of Peierls for a constructed distribution without precession and with precession in a field of 7 gauss (period 10.55 μsec) confirms that (18) is approximately correct.

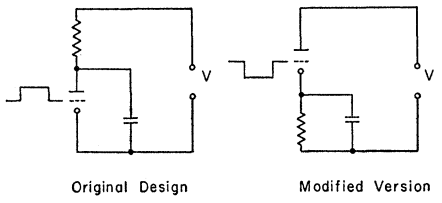

FIG. 4. Essential features of the time-to-pulse-height converter. The original version is that of reference 17.

[19] R. Peierls, Proc. Roy. Soc. (London) **A149**, 467 (1935).

[20] Garwin, Lederman, and Weinrich, Phys. Rev. **105**, 1415 (1957); J. I. Friedman and V. L. Telegdi, Phys. Rev. **105**, 1681 (1957).

[21] It is to be noted that in (17), $\tilde{\Lambda}_t$ is a function of t.

TABLE I. Capture rates calculated from the experimental data.

Element[a] (I)	No. of analyzed electrons (II)	Rate/backgr. in 1° interval (β) (III)	T/τ[d] (IV)	Λ_t observed (10^5 sec^{-1}) (V)	$\Delta\Lambda_t$[e] (10^5 sec^{-1}) (VI)	Corrected lifetime τ^- (10^{-6} sec) (VII)	Corrected capture rate Λ_{cap} (10^5 sec^{-1}) (VIII)
Be	71755	13	2.70	4.55±0.05	0.13	2.14 ±0.02	0.18±0.10
C	62817	11	2.96	4.69±0.06	0.25	2.02 ±0.02	0.44±0.10
N	47029	18	2.86	5.15±0.06	0.21	1.86 ±0.02	0.86±0.11
O(H_2)	12460	9.2	3.40	5.88±0.11	0.21	1.64 ±0.03	1.59±0.14
F(KH)$_4$	41337[c]	···	···	6.94±0.18	···	1.42 ±0.04	2.54±0.22
Na	29346	29.5	4.28	8.26±0.11	0.11	1.19 ±0.02	3.87±0.15
Mg	29455	9.7	5.21	9.36±0.16	0.21	1.04 ±0.02	5.07±0.20
Al	82083	24.7	3.10	11.32±0.16	0.09	0.88 ±0.01	6.91±0.20
Si	34919	17.4	3.56	12.06±0.21	0.21	0.81 ±0.01	7.77±0.25
P	8485	7.2	4.38	14.92±0.46	0.21	0.66 ±0.02	10.54±0.50
S	22773	30	4.0	18.2 ±0.9	0.24	0.54 ±0.02	13.9 ±0.9
Cl(Na)	3762[c]	···	···	18.3 ±0.9	···	0.54 ±0.02	13.9 ±0.9
K(OH)	5890[c]	···	···	24.4 ±1.2	···	0.41 ±0.02	19.9 ±1.2
Ca	25118	10.2	3.0	29.6 ±0.5	0.41	0.333±0.007	25.5 ±0.5
Ti	26185	15.2	3.0	30.3 ±0.6	0.50	0.330±0.007	26.3 ±0.6
V	24423	16.6	3.9	37.9 ±0.6	0.34	0.264±0.004	33.7 ±0.6
Cr	12651	7.8	3.7	36.2 ±0.8	0.69	0.276±0.006	32.4 ±0.8
Mn	16509	1.7	4.3	41.8 ±0.8	0.41	0.239±0.004	36.7 ±0.8
Fe	20455	17.4	3.0	49.4 ±1.0	0.39	0.201±0.004	45.3 ±1.0
Ni	10209	12.6	4.5	64.1 ±1.4	0.68	0.154±0.003	60.3 ±1.4
Cu[b]	14548	42.8	3.2	62.1 ±1.6	0.29	0.160±0.004	57.9 ±1.6
Zn[b]	4542	25	3.6	62.1 ±1.6	···	0.161±0.004	57.6 ±1.7
Mo[b]	10441	25	4.0	95.2 ±1.8	0.24	0.105±0.002	90.9 ±1.8
Ag	3018	7.7	3.9	116.5 ±5.0	0.49	(85±3)×10^{-3}	112.5 ±5.0
Cd	2759	7.0	4.0	104.5 ±5.0	0.46	(95±5)×10^{-3}	100.5 ±5.0
W[b]	9654	17.5	4.0	123.5 ±3.0	0.18	(81±2)×10^{-3}	119.2 ±3.0
Tl	1804	6.0	4.0	133.0 ±7.5	0.49	(75±4)×10^{-3}	129.0 ±7.5
Pb	3981	4.1	4.0	121.5 ±7.5	0.29	(82±5)×10^{-3}	117.0 ±7.5
Bi	1457	4.9	3.2	126.5 ±7.5	0.44	(79±5)×10^{-3}	122.0 ±7.5
U	2565	5.7	3.5	113.5 ±5.0	0.57	(88±4)×10^{-3}	109.0 ±5.0

[a] Other constituents are indicated in parentheses where the target was a compound.
[b] These elements were measured in an improved arrangement (see text). In the case of Cu, the data from the "old" and the "new" arrangement were combined.
[c] Number of electrons calculated from the stoichiometric ratios for muons stopping in the elements of the compound. See reference 23.
[d] T = total time over which analysis is extended. τ = observed mean life.
[e] $\Delta\Lambda_t$ = sum of corrections (1) and (2) (see text).

Under the conditions of the present experiment, the cyclotron stray field produced a vertical component at the location of the target of about 7 gauss. The asymmetry coefficient, a, for negative muons has been measured for various substances[22] and found to be about 0.04. The correction ranges from 3% ($Z=4$) to 1% ($Z=16$), is negligible for higher Z, and is zero for all nuclei with nonzero nuclear spin. Since the electron distribution is peaked backwards with respect to the momentum of the muon, the correction $\Delta\Lambda_t$ must be added to the observed Λ_t.

As a final correction, the effect of atomic binding on the muon decay rate, Λ_d^-, has been considered. For the elements for which R has been measured,[13] the correction to Λ_{cap} never exceeds 2%. In view of its smallness and the fact that a more detailed investigation of this effect is still in progress, we have omitted this correction.

Table I gives a summary of the information pertinent to the evaluation of the capture rates and the errors. The data obtained with compound targets were evaluated by a least-squares fit. Four elements were measured in an arrangement which differs from that of Fig. 2 in that a collimator of 3-in. diameter was used and two counters, instead of one, were placed behind the absorber. This results in a considerable reduction in background, as is apparent from the β values in the table.

[22] Ignatanko, Egorov, Halupa, and Chultem (private communication).

C. Detection of Nuclear Gamma Rays

Prior to the experiment described above, we obtained evidence on the capture of muons by nuclei in measurements which formed part of a study of the energies and relative intensities of μ-mesonic x-rays in Pb. In these measurements, the time distribution of the nuclear gamma rays following muon capture was measured in the following manner: Muons were made to stop in a 10-g/cm^2 Pb target. The emerging nuclear gamma rays traverse a plastic scintillator having low sensitivity for counting gamma rays and enter a 5-in. diam NaI crystal, see Fig. 5. The stopped muon is identified by a (1,2) coincidence, the μ-mesonic x-ray or nuclear γ ray by a $(1,2,\bar{3},X)$ event. To be able to make a fast coincidence in the $(1,2,\bar{3},X)$ telescope, the crystal pulse (X) is taken from a dynode of the 5-in. DuMont photomultiplier and fed into a limiter-clipper before entering the coincidence circuit. The "energy" threshold of the limiter-clipper is determined by

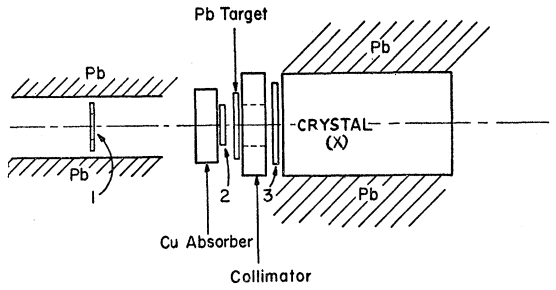

FIG. 5. Experimental arrangement for the detection of mesonic x-rays and nuclear γ rays. Nuclear γ ray $(12\bar{3}X)$; monitor (1,2).

placing a Na^{23} source at the location of the target and analyzing the photomultiplier anode signal with the P.H.A., the input of which is gated by a $(\bar{3},X)$ coincidence. The threshold is such that only x-rays and nuclear gamma rays of energies >350 kev are detectable. By varying the delay of X with respect to $(1,2,\bar{3})$, one obtains a time distribution as shown in Fig. 6. The capture mean life deduced is 72 ± 10 mμsec, while the integrated contributions of the nuclear gamma rays and the x-rays are in the ratio 0.46 ± 0.05. Assuming 6–7 x-rays per stopped muon, this leads to about three gamma rays per muon captured in lead, in agreement with cloud chamber evidence.[24]

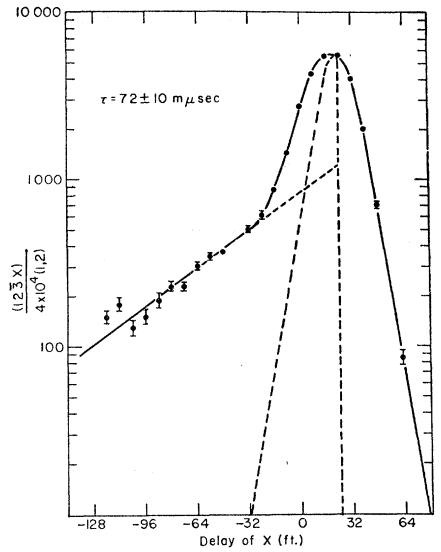

FIG. 6. Delay curve, obtained with the arrangement of Fig. 5.

III. DISCUSSION OF THE RESULTS

A. The Effective Nuclear Charge Density

As mentioned in Sec. IA, Z_{eff}, and thus $\langle\rho\rangle$, have been evaluated by Wheeler using harmonic oscillator muon wave functions both inside and outside the nuclear surface.

To obtain more accurate values for $\langle\rho\rangle$, we have employed the available experimental information on both the $2p-1s$ transition energies in μ-mesonic atoms[25] (x-ray data) and the scattering of fast electrons by nuclei[26] (scattering data) to determine the nuclear charge distributions and the muon wave functions. The procedure is as follows: from the electron scattering data on various nuclei it appears that their charge distributions can be represented by a Fermi-type function, which we write in the form given by Hill and Ford[27]:

$$\rho(x)=\frac{\rho_0}{1-0.5e^{-n}}\begin{cases}1-0.5e^{-n(1-x)}, & x\leqslant 1\\ 0.5e^{-n(x-1)}, & x\geqslant 1\end{cases} \tag{19}$$

where ρ_0=charge density at the center of the nucleus, n is a shape parameter, and $x=r/R$; R is the range parameter, which defines the radial extent of the charge.[28] The nuclei investigated here may now be divided into three classes:

(A) Nuclei for which a shape specified as to n as well as to R is available from scattering data. The Dirac equation with the potential following from (19) can then be solved numerically; from the $1s$-state wave function $\langle\rho\rangle$ is found. Since x-ray data are available for some nuclei in this class, the consistency of the two types of experiments can be checked.

(B) Nuclei for which x-ray data but no scattering data are available. Assuming shape (19), n is first estimated from an approximate radius R and "skin thickness" t, and R is varied so that the computed $2p-1s$ transition energy agrees with the experimental value.

(C) Nuclei for which neither x-ray nor scattering data are available. Here R is computed from $R=r_0(A)A^{\frac{1}{3}}$ and n is computed from this R and an interpolated value of t.

The charge distributions, thus obtained, were inserted into an existing[29] IBM-704 computer code, which calculated the solutions of the Dirac equation for the corresponding potentials, the $2p-1s$ transition energy, and $\langle\rho\rangle$.

Table II summarizes the relevant quantities.

B. Comparison of Experiment with Theory

In order to compare the measured capture rates with the predictions of the universal Fermi interaction

[23] Sens, Swanson, Telegdi, and Yovanovitch, Nuovo cimento **7**, 536 (1958).
[24] W. Y. Chang, Revs. Modern Phys. **21**, 166 (1949); T. J. B. Shanley, thesis, Princeton University, 1951 (unpublished).
[25] V. L. Fitch and J. Rainwater, Phys. Rev. **92**, 789 (1953); M. B. Stearns and M. Stearns, Phys. Rev. **105**, 1573 (1957).
[26] R. Hofstadter, *Annual Review of Nuclear Science* (Annual Reviews, Inc., Stanford, 1957), Vol. 7, p. 301.
[27] D. L. Hill and K. W. Ford, Phys. Rev. **94**, 1617 (1954).
[28] For $Z<10$, other distributions compatible with experiment exist.
[29] This code was set up by D. L. Hill and K. W. Ford for the calculations of reference 27. It was extended to include the calculation of $\langle\rho\rangle$.

TABLE II. Effective charge densities.

Element (I)	A (II)	$r_0=R/A^{\frac{1}{3}}$ (fermi) (III)	$\gamma=R/\lambda\!\!\!^{-}_{\mu}$ [a] (IV)	n [b] (V)	$E_{2p_{3/2}-1s}$ (Mev) Point nucleus values (VI)	Finite nucleus values (VII)	Experimental values (VIII)	$\langle\rho\rangle$ (protons/fermi^3) (IX)	Z_{eff} [c] (X)	Wheeler's Z_{eff} [d] (XI)
					CLASS A					
Be	9.00	0.83	0.925	2.25	0.03336	0.03328	0.0333	4.528×10^{-6}	3.97	3.93
C	12.01	1.009	1.238	3.0	0.07532	0.07478	0.0750	2.026×10^{-5}	5.75	5.78
O	16.00	1.045	1.411	3.5	0.1343	0.1325	0.1330	2.786×10^{-5}	7.47	7.56
Mg	24.32	1.03	1.596	3.5	0.3033	0.2927	0.295	2.478×10^{-4}	10.72	10.83
Si	28.11	1.03	1.677	3.8	0.4134	0.3946	0.410	4.265×10^{-4}	12.27	12.31
S	32.08	1.04	1.768	4.0	0.5407	0.5087	···	6.612×10^{-4}	13.69	13.7
Ca	40.10	1.063	1.949	4.1	0.8476	0.7664	···	1.290×10^{-3}	16.17	16.2
V	51.00	1.057	2.099	5.0	1.1240	0.9940	···	2.016×10^{-3}	18.07	17.9
Ni	58.77	1.06	2.207	5.0	1.6736	···	···	3.462×10^{-3}	20.69	20.3
Pb	207.8	1.11	3.520	10.0	16.161	5.987	6.02	2.592×10^{-2}	34.18	31.4
Bi	209.0	1.094	3.478	7.7	16.621	5.959	6.02	2.542×10^{-2}	34.02	31.5
					CLASS B					
N	14.00	1.02	1.317	3.2	0.1027	0.1016	0.102	3.532×10^{-5}	6.60	6.68
F	19.00	1.03	1.472	3.5	0.1702	0.1671	0.168	8.969×10^{-5}	8.32	8.40
Na	23.00	1.03	1.569	3.7	0.2547	0.2477	0.249	1.867×10^{-4}	9.99	10.02
Al	27.00	1.03	1.655	3.8	0.3562	0.3423	0.35	3.287×10^{-4}	11.50	11.58
P	31.00	1.04	1.750	3.9	0.4750	0.4495	0.470	5.326×10^{-4}	12.97	13.02
Cl	35.49	1.05	1.848	4.0	0.6110	0.5682	0.590	7.830×10^{-4}	14.28	14.4
K	39.14	1.06	1.928	4.1	0.7644	0.6978	0.730	1.105×10^{-3}	15.56	15.6
Ti	47.93	1.06	2.063	4.6	1.0275	0.9135	0.955	1.734×10^{-3}	17.41	17.4
Cu	63.62	1.07	2.288	5.4	1.7973	1.4870	1.55	3.789×10^{-3}	21.16	20.7
Zn	65.48	1.07	2.310	5.5	1.9255	1.576	1.60	4.162×10^{-3}	21.66	21.1
					CLASS C					
Cr	52.06	1.07	2.140	4.8	1.2249	1.0667	···	2.225×10^{-3}	18.53	18.4
Mn	55.00	1.07	2.178	5.0	1.3304	1.1480	···	2.518×10^{-3}	19.11	18.9
Fe	55.93	1.07	2.192	5.0	1.4403	1.230	···	2.805×10^{-3}	19.63	19.4
Mo	95.98	1.08	2.649	6.8	3.834	2.695	···	9.189×10^{-3}	26.39	25.2
Ag	107.97	1.08	2.755	7.2	4.840	3.177	···	1.162×10^{-2}	27.98	26.2
Cd	112.52	1.08	2.793	7.4	5.057	3.269	···	1.204×10^{-2}	28.23	26.5
W	184.0	1.10	3.352	7.5	12.802	5.326	···	2.190×10^{-2}	32.77	30.7
Tl	204.4	1.10	3.471	9.9	15.711	5.962	···	2.605×10^{-2}	34.22	31.3
U	238.0	1.10	3.652	8.5	21.218	6.500	···	2.832×10^{-2}	34.95	32.2

[a] $\lambda\!\!\!^{-}_{\mu}$ = moun Compton wavelength $=1.8667\times\mu^{-1}$; μ is a reduced-mass correction factor: $\mu=A/(A+0.1137)$; $m_\mu=206.86m_e\times\mu$.
[b] Shape parameter of (19) in text.
[c] Z_{eff}, obtained from $\langle\rho\rangle$ and (3) in text, but using $a_0(A)=a_0(\infty)\mu$, the reduced Bohr radius for a nucleus of mass A; rather than $a_0(\infty)$; see reference 30.
[d] Z_{eff}, obtained from (4) in text.

(UFI), we write for the capture rate of protons by muons[30] $\Lambda_{\text{cap}}(1,1)=K^2/\pi a_0^3$. With this notation and (3), Primakoff's expression (7) becomes

$$\Lambda_{\text{cap}}(Z,A)=\gamma K^2\langle\rho\rangle[1-\delta(A-Z)/2A]. \tag{20}$$

Figure 7 shows a plot of $\Lambda_{\text{cap}}(Z,A)/\langle\rho\rangle$ *versus* $(A-Z)/2A$, derived using the data of Tables I and II. Omitting the data for O^{16} and F^{19} (because of uncertainties connected with the fact that the rates for these nuclei were obtained from measurements with compound targets), a weighted least-squares fit of (20) to the experimental points was made. It yields the straight line indicated in Fig. 7, corresponding to the parameters

$$\gamma K^2=98.92\times10^{-31}\ \text{cm}^3\ \text{sec}^{-1},\qquad \delta=3.15. \tag{21}$$

Thus one obtains

$$\gamma\Lambda_{\text{cap}}(1,1)=188\ \text{sec}^{-1}.\quad\text{(experimental)} \tag{22}$$

TABLE III. Theoretical capture rates for S,V and T,A interactions, compared with experiment.

	S,V a	S,V b	T,A a	T,A b	Equal amounts of S,V and T,A a	Equal amounts of S,V and T,A b	Experimental values
Ti/Ca	0.88	0.94	1.01	1.13	0.98	1.08	1.03±0.03
V/Ca	0.77	0.79	1.03	1.19	0.96[5]	1.09	1.32±0.04
Cr/Ca	0.90	0.94	1.28	1.49	1.18	1.35	1.27±0.04
Mn/Ca	0.94[5]	0.99	1.43	1.71	1.31	1.53	1.44±0.05
Fe/Ca	1.08	1.14	1.70	2.05	1.54[5]	1.82	1.78±0.06
Ni/Ca	1.34	1.42	2.21	2.77	1.99	2.43	2.36±0.07

[a] $r_0=1.40\times10^{-13}$ cm.
[b] $r_0=1.15\times10^{-13}$ cm.

[30] It is to be emphasized once more that $\Lambda(1,1)$ is not the actual rate for absorption of muons from the K orbit around protons. This latter rate is given by $\Lambda_{\text{cap}}^{\text{phys}}(1,1)=K^2/\pi a_0^3(1)$, with $a_0(A)=$*reduced* Bohr radius for a nucleus of mass A. Also a better definition of Z_{eff}^4 than (3) is $\tilde{Z}_{\text{eff}}^4=\pi a_0^3(A)\langle\rho\rangle$. For $Z=1$, $\tilde{Z}_{\text{eff}}=1$, while $Z_{\text{eff}}=1[a_0(\infty)/a_0(1)]^3$. In terms of these variables, (7) reads $\Lambda_{\text{cap}}(Z,A)=\Lambda_{\text{cap}}^{\text{phys}}(1,1)\times[a_0(1)/a_0(A)]^3Z_{\text{eff}}^4[1-\delta\times(A-Z)/2A]$. Table II lists what we call here Z_{eff}; except for the lightest nuclei, $\tilde{Z}_{\text{eff}}=Z_{\text{eff}}$.

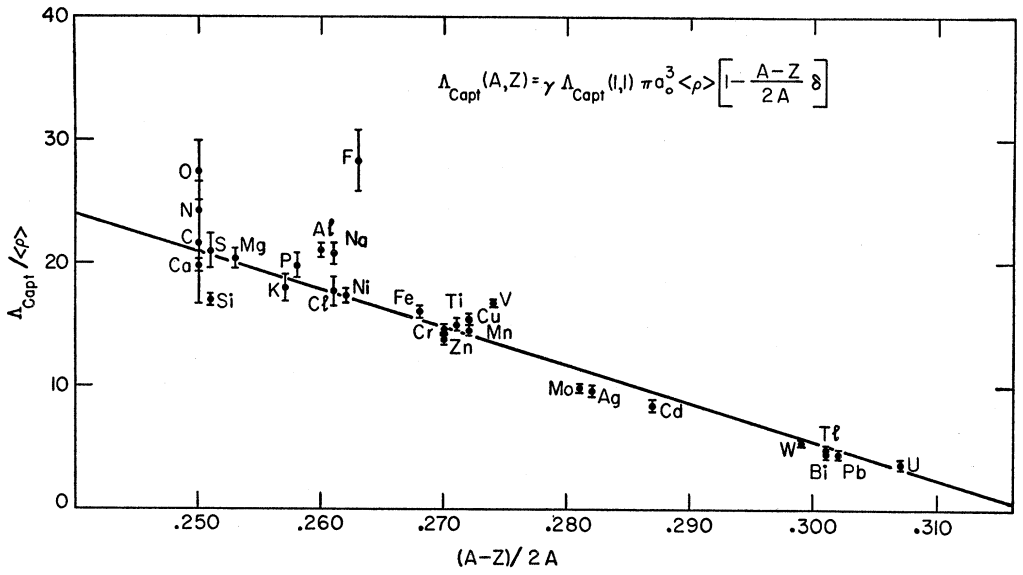

FIG. 7. Plot of $\Lambda_{cap}(A,Z)/\langle\rho\rangle$ *versus* $(A-Z)/2A$, showing the effect of the Pauli principle. The line is a weighted least-squares fit to the observed data.

The statistical error on this quantity is about 1.5%, but it need not represent the total uncertainty and for this reason we quote no error in (22). From (9) and Primakoff's estimate $\gamma=0.73$, to which he assigns an uncertainty of $\pm 20\%$, we obtain

$$\gamma\Lambda_{cap}(1,1)=(153\pm 30)\ \text{sec}^{-1}, \quad \text{(theoretical)} \quad (22')$$

assuming UFI to hold. Thus this assumption is as well supported by the result of the present experiment as can be expected in view of the inherent limitations of the theory, at least as far as the equality of the effective coupling strengths $\sum c_i^2$ [see Eq. (6)] is concerned. This equality suggests that two-component neutrinos are involved in muon capture, a process for which parity nonconservation had as yet not been established experimentally.

The agreement between (22) and (22′) concerns, however, only the strengths of the couplings and does not supply any evidence that their detailed structure, e.g., the ratio of Gamow-Teller to Fermi type interactions, is also universal. According to Tolhoek and Luyten,[11] who have performed specific shell model calculations assuming pure Fermi (S,V) or Gamow-Teller (T,A) interactions and two different sets of values for the nuclear radii, such information could be derived from the observed muon capture rates (or rather their ratios) of nuclei in the range $20\leq Z\leq 28$. The predictions of these authors are compared with the present experimental results in Table III. The observed ratios are in reasonable agreement, provided one adopts the "small" radii, with the predictions for equal amounts of Fermi and Gamow-Teller interactions, although a pure Gamow-Teller interaction, with "large" radii, cannot be excluded. Thus the experimental evidence, though inconclusive, is at least consistent with the $V-A$ interaction now favored in the interpretation of weak interactions.[6]

IV. ACKNOWLEDGMENTS

I am indebted to Professor V. L. Telegdi for suggesting this experiment and for his guidance during the course of this research. I wish to thank R. A. Swanson and D. D. Yovanovitch for assistance in the preparation and performance of the experiment. The excellent cooperation of Dr. K. W. Ford and collaborators at the Los Alamos Scientific Laboratories in the calculation of the charge densities is gratefully acknowledged.